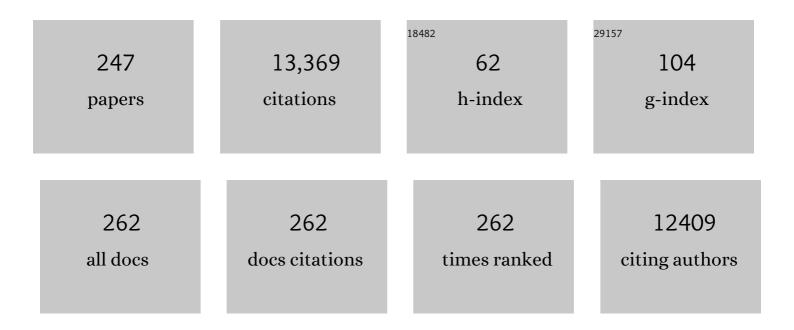
List of Publications by Year in descending order

Source: https://exaly.com/author-pdf/1344533/publications.pdf Version: 2024-02-01



ΔΜΙΤ ΚΙΙΜΛΟ

#	Article	IF	CITATIONS
1	Novel development of nanoparticles to bimetallic nanoparticles and their composites: A review. Journal of King Saud University - Science, 2019, 31, 257-269.	3.5	431
2	The ins and outs of microorganism–electrode electron transfer reactions. Nature Reviews Chemistry, 2017, 1, .	30.2	385
3	Quaternary magnetic BiOCl/g-C3N4/Cu2O/Fe3O4 nano-junction for visible light and solar powered degradation of sulfamethoxazole from aqueous environment. Chemical Engineering Journal, 2018, 334, 462-478.	12.7	311
4	Guar gum and its composites as potential materials for diverse applications: A review. Carbohydrate Polymers, 2018, 199, 534-545.	10.2	283
5	<scp>DNA</scp> barcoding: an efficient tool to overcome authentication challenges in the herbal market. Plant Biotechnology Journal, 2016, 14, 8-21.	8.3	255
6	Construction of dual Z-scheme g-C3N4/Bi4Ti3O12/Bi4O5I2 heterojunction for visible and solar powered coupled photocatalytic antibiotic degradation and hydrogen production: Boosting via lâ^'/I3â^' and Bi3+/Bi5+ redox mediators. Applied Catalysis B: Environmental, 2021, 284, 119808.	20.2	252
7	Biochar-templated g-C3N4/Bi2O2CO3/CoFe2O4 nano-assembly for visible and solar assisted photo-degradation of paraquat, nitrophenol reduction and CO2 conversion. Chemical Engineering Journal, 2018, 339, 393-410.	12.7	241
8	Magnetic polymer nanocomposites for environmental and biomedical applications. Colloid and Polymer Science, 2014, 292, 2025-2052.	2.1	228
9	Sustainable nano-hybrids of magnetic biochar supported g-C 3 N 4 /FeVO 4 for solar powered degradation of noxious pollutants- Synergism of adsorption, photocatalysis & photo-ozonation. Journal of Cleaner Production, 2017, 165, 431-451.	9.3	219
10	Fabrication and characterization of chitosan-crosslinked-poly(alginic acid) nanohydrogel for adsorptive removal of Cr(VI) metal ion from aqueous medium. International Journal of Biological Macromolecules, 2017, 95, 484-493.	7.5	217
11	Applications of nanocomposite hydrogels for biomedical engineering and environmental protection. Environmental Chemistry Letters, 2018, 16, 113-146.	16.2	207
12	Bio-inspired and biomaterials-based hybrid photocatalysts for environmental detoxification: A review. Chemical Engineering Journal, 2020, 382, 122937.	12.7	201
13	Photocatalytic degradation of highly toxic dyes using chitosan-g-poly(acrylamide)/ZnS in presence of solar irradiation. Journal of Photochemistry and Photobiology A: Chemistry, 2016, 329, 61-68.	3.9	196
14	Revolution from monometallic to trimetallic nanoparticle composites, various synthesis methods and their applications: A review. Materials Science and Engineering C, 2017, 71, 1216-1230.	7.3	195
15	Wide spectral degradation of Norfloxacin by Ag@BiPO4/BiOBr/BiFeO3 nano-assembly: Elucidating the photocatalytic mechanism under different light sources. Journal of Hazardous Materials, 2019, 364, 429-440.	12.4	193
16	Efficient removal of coomassie brilliant blue R-250 dye using starch/poly(alginic acid-cl-acrylamide) nanohydrogel. Chemical Engineering Research and Design, 2017, 109, 301-310.	5.6	183
17	Fabrication and characterization of Gum arabic-cl-poly(acrylamide) nanohydrogel for effective adsorption of crystal violet dye. Carbohydrate Polymers, 2018, 202, 444-453.	10.2	174
18	Solar photocatalytic activity of nano-ZnO supported on activated carbon or brick grain particles: Role of adsorption in dye degradation. Applied Catalysis A: General, 2014, 486, 159-169.	4.3	164

#	Article	IF	CITATIONS
19	Two analytical methods for time-fractional nonlinear coupled Boussinesq–Burger's equations arise in propagation of shallow water waves. Nonlinear Dynamics, 2016, 85, 699-715.	5.2	164
20	Facile hetero-assembly of superparamagnetic Fe3O4/BiVO4 stacked on biochar for solar photo-degradation of methyl paraben and pesticide removal from soil. Journal of Photochemistry and Photobiology A: Chemistry, 2017, 337, 118-131.	3.9	158
21	Nano Fe x Zn 1â^'x O as a tuneable and efficient photocatalyst for solar powered degradation of bisphenol A from aqueous environment. Journal of Cleaner Production, 2017, 165, 1542-1556.	9.3	157
22	Integrated bioprocess for conversion of gaseous substrates to liquids. Proceedings of the National Academy of Sciences of the United States of America, 2016, 113, 3773-3778.	7.1	156
23	Highly efficient Sr/Ce/activated carbon bimetallic nanocomposite for photoinduced degradation of rhodamine B. Catalysis Today, 2019, 335, 437-451.	4.4	155
24	Fabrication and characterization of novel Fe0@Guar gum-crosslinked-soya lecithin nanocomposite hydrogel for photocatalytic degradation of methyl violet dye. Separation and Purification Technology, 2019, 211, 895-908.	7.9	152
25	Photoremediation of toxic dye from aqueous environment using monometallic and bimetallic quantum dots based nanocomposites. Journal of Cleaner Production, 2018, 172, 2919-2930.	9.3	140
26	High-Performance Photocatalytic Hydrogen Production and Degradation of Levofloxacin by Wide Spectrum-Responsive Ag/Fe <sub>3</sub> O <sub>4</sub> Bridged SrTiO <sub>3</sub> /g-C <sub>3</sub> N <sub>4</sub> Plasmonic Nanojunctions: Joint Effect of Ag and Fe <sub>3</sub> O <sub>4</sub> . ACS Applied Materials & Interfaces, 2018, 10, 40474-40490.	8.0	140
27	SPION/β-cyclodextrin core–shell nanostructures for oil spill remediation and organic pollutant removal from waste water. Chemical Engineering Journal, 2015, 280, 175-187.	12.7	137
28	Removal of malachite green and methylene blue by Fe0.01Ni0.01Zn0.980/polyacrylamide nanocomposite using coupled adsorption and photocatalysis. Applied Catalysis B: Environmental, 2014, 147, 340-352.	20.2	135
29	Impact of heavy metals and nanoparticles on aquatic biota. Environmental Chemistry Letters, 2018, 16, 919-946.	16.2	127
30	Highly visible active Ag2CrO4/Ag/BiFeO3@RGO nano-junction for photoreduction of CO2 and photocatalytic removal of ciprofloxacin and bromate ions: The triggering effect of Ag and RGO. Chemical Engineering Journal, 2019, 370, 148-165.	12.7	126
31	Recent advances in nano-Fenton catalytic degradation of emerging pharmaceutical contaminants. Journal of Molecular Liquids, 2019, 290, 111177.	4.9	120
32	Fabrication and characterization of trimetallic nano-photocatalyst for remediation of ampicillin antibiotic. Journal of Molecular Liquids, 2018, 260, 342-350.	4.9	119
33	Biodegradable and conducting hydrogels based on Guar gum polysaccharide for antibacterial and dye removal applications. Journal of Environmental Management, 2015, 162, 37-45.	7.8	117
34	Magnetically recoverable ZrO <sub>2</sub> /Fe <sub>3</sub> O <sub>4</sub> /chitosan nanomaterials for enhanced sunlight driven photoreduction of carcinogenic Cr( <scp>vi</scp> ) and dechlorination & mineralization of 4-chlorophenol from simulated waste water. RSC Advances, 2016, 6, 13251-13263.	3.6	115
35	Fe3O4/ZnO/Si3N4 nanocomposite based photocatalyst for the degradation of dyes from aqueous solution. Materials Letters, 2020, 278, 128359.	2.6	115
36	Polyacrylamide/Ni <sub>0.02</sub> Zn <sub>0.98</sub> O Nanocomposite with High Solar Light Photocatalytic Activity and Efficient Adsorption Capacity for Toxic Dye Removal. Industrial & Engineering Chemistry Research, 2014, 53, 15549-15560.	3.7	113

#	Article	IF	CITATIONS
37	Efficient removal of toxic phosphate anions from aqueous environment using pectin based quaternary amino anion exchanger. International Journal of Biological Macromolecules, 2018, 106, 1-10.	7.5	112
38	Polyacrylamide@Zr(IV) vanadophosphate nanocomposite: Ion exchange properties, antibacterial activity, and photocatalytic behavior. Journal of Industrial and Engineering Chemistry, 2016, 33, 201-208.	5.8	102
39	Adsorptional-photocatalytic removal of fast sulphon black dye by using chitin-cl-poly(itaconic) Tj ETQq1 1 0.78431 2021, 416, 125714.	.4 rgBT /O <sup>.</sup> 12.4	verlock 10 102
40	ZnSe-WO3 nano-hetero-assembly stacked on Gum ghatti for photo-degradative removal of Bisphenol A: Symbiose of adsorption and photocatalysis. International Journal of Biological Macromolecules, 2017, 104, 1172-1184.	7.5	101
41	Microwave assisted fabrication of La/Cu/Zr/carbon dots trimetallic nanocomposites with their adsorptional vs photocatalytic efficiency for remediation of persistent organic pollutants. Journal of Photochemistry and Photobiology A: Chemistry, 2017, 347, 235-243.	3.9	100
42	Guar gum-crosslinked-Soya lecithin nanohydrogel sheets as effective adsorbent for the removal of thiophanate methyl fungicide. International Journal of Biological Macromolecules, 2018, 114, 295-305.	7.5	100
43	Visible photodegradation of ibuprofen and 2,4-D in simulated waste water using sustainable metal free-hybrids based on carbon nitride and biochar. Journal of Environmental Management, 2019, 231, 1164-1175.	7.8	100
44	CeO2/g-C3N4/V2O5 ternary nano hetero-structures decorated with CQDs for enhanced photo-reduction capabilities under different light sources: Dual Z-scheme mechanism. Journal of Alloys and Compounds, 2020, 838, 155692.	5.5	96
45	Silicate glass matrix@Cu2O/Cu2V2O7 p-n heterojunction for enhanced visible light photo-degradation of sulfamethoxazole: High charge separation and interfacial transfer. Journal of Hazardous Materials, 2021, 402, 123790.	12.4	95
46	Sodium Hydroxide Production from Seawater Desalination Brine: Process Design and Energy Efficiency. Environmental Science & Technology, 2018, 52, 5949-5958.	10.0	94
47	Magnetic Cellulose Nanocrystal Based Anisotropic Polylactic Acid Nanocomposite Films: Influence on Electrical, Magnetic, Thermal, and Mechanical Properties. ACS Applied Materials & Interfaces, 2016, 8, 18393-18409.	8.0	93
48	Facile synthesis of mesoporous NiFe 2 O 4 /CNTs nanocomposite cathode material for high performance asymmetric pseudocapacitors. Applied Surface Science, 2018, 433, 1100-1112.	6.1	92
49	Lithium Recovery from Oil and Gas Produced Water: A Need for a Growing Energy Industry. ACS Energy Letters, 2019, 4, 1471-1474.	17.4	92
50	Fabrication and characterization of Fe@MoPO nanoparticles: Ion exchange behavior and photocatalytic activity against malachite green. Journal of Molecular Liquids, 2016, 219, 1137-1143.	4.9	90
51	Solar-driven photodegradation of 17-Î <sup>2</sup> -estradiol and ciprofloxacin from waste water and CO <sub>2</sub> conversion using sustainable coal-char/polymeric-g-C <sub>3</sub> N <sub>4</sub> /RGO metal-free nano-hybrids. New Journal of Chemistry, 2017, 41, 10208-10224.	2.8	90
52	Molecular Basis of Enrofloxacin Translocation through OmpF, an Outer Membrane Channel of Escherichia coli - When Binding Does Not Imply Translocation. Journal of Physical Chemistry B, 2010, 114, 5170-5179.	2.6	88
53	Rapid visible and solar photocatalytic Cr(VI) reduction and electrochemical sensing of dopamine using solution combustion synthesized ZnO–Fe2O3 nano heterojunctions: Mechanism Elucidation. Ceramics International, 2020, 46, 12255-12268.	4.8	87
54	Solar-Fenton removal of malachite green with novel FeO-activated carbon nanocomposite. Applied Catalysis A: General, 2014, 476, 9-18.	4.3	81

#	Article	IF	CITATIONS
55	Fabrication and characterization of sodium dodecyl sulphate@ironsilicophosphate nanocomposite: Ion exchange properties and selectivity for binary metal ions. Materials Chemistry and Physics, 2017, 193, 129-139.	4.0	79
56	Utilization of Desalination Brine for Sodium Hydroxide Production: Technologies, Engineering Principles, Recovery Limits, and Future Directions. ACS Sustainable Chemistry and Engineering, 2017, 5, 11147-11162.	6.7	79
57	Pectin-c rosslinked -guar gum/SPION nanocomposite hydrogel for adsorption of m-cresol and o-chlorophenol. Sustainable Chemistry and Pharmacy, 2017, 6, 96-106.	3.3	78
58	Efficiency of ISSR and RAPD markers in genetic divergence analysis and conservation management of Justicia adhatoda L., a medicinal plant. Plant Systematics and Evolution, 2014, 300, 1409-1420.	0.9	76
59	Atrazine removal using chitin-cl-poly(acrylamide-co-itaconic acid) nanohydrogel: Isotherms and pH responsive nature. Carbohydrate Polymers, 2020, 241, 116258.	10.2	74
60	Zero valent iron-brick grain nanocomposite for enhanced solar-Fenton removal of malachite green. Separation and Purification Technology, 2014, 133, 429-437.	7.9	70
61	Lanthanum/Cadmium/Polyaniline bimetallic nanocomposite for the photodegradation of organic pollutant. Iranian Polymer Journal (English Edition), 2015, 24, 1003-1013.	2.4	70
62	Fabrication and characterization of a nanocomposite hydrogel for combined photocatalytic degradation of a mixture of malachite green and fast green dye. Nanotechnology for Environmental Engineering, 2017, 2, 1.	3.3	70
63	ZnO-based heterostructures as photocatalysts for hydrogen generation and depollution: a review. Environmental Chemistry Letters, 2022, 20, 1047-1081.	16.2	68
64	Direct electrosynthesis of sodium hydroxide and hydrochloric acid from brine streams. Nature Catalysis, 2019, 2, 106-113.	34.4	65
65	Adsorptional removal of methylene blue by guar gum–cerium (IV) tungstate hybrid cationic exchanger. Carbohydrate Polymers, 2014, 101, 684-691.	10.2	64
66	Assessment of landslide hazards induced by extreme rainfall event in Jammu and Kashmir Himalaya, northwest India. Geomorphology, 2017, 284, 72-87.	2.6	64
67	Synthesis and characterization of a new nanocomposite cation exchanger polyacrylamide Ce(IV) silicophosphate: Photocatalytic and antimicrobial applications. Journal of Industrial and Engineering Chemistry, 2014, 20, 3596-3603.	5.8	63
68	Fabrication of nanocomposite polyaniline zirconium(IV) silicophosphate for photocatalytic and antimicrobial activity. Journal of Alloys and Compounds, 2014, 588, 668-675.	5.5	62
69	Combined sorptional–photocatalytic remediation of dyes by polyaniline Zr(IV) selenotungstophosphate nanocomposite. Toxicological and Environmental Chemistry, 2015, 97, 526-537.	1.2	62
70	Algal biochar reinforced trimetallic nanocomposite as adsorptional/photocatalyst for remediation of malachite green from aqueous medium. Journal of Molecular Liquids, 2019, 275, 499-509.	4.9	62
71	Twoâ€Ðimensional Layered Materials as Catalyst Supports. ChemNanoMat, 2018, 4, 28-40.	2.8	61
72	Metals Recovery from Seawater Desalination Brines: Technologies, Opportunities, and Challenges. ACS Sustainable Chemistry and Engineering, 2021, 9, 7704-7712.	6.7	60

#	Article	IF	CITATIONS
73	Carbon quantum dots and reduced graphene oxide modified self-assembled S@C3N4/B@C3N4 metal-free nano-photocatalyst for high performance degradation of chloramphenicol. Journal of Molecular Liquids, 2020, 300, 112356.	4.9	59
74	Preparation of BSA-ZnWO <sub>4</sub> Nanocomposites with Enhanced Adsorptional Photocatalytic Activity for Methylene Blue Degradation. International Journal of Photoenergy, 2013, 2013, 1-7.	2.5	58
75	Robust magnetic ZnO-Fe2O3 Z-scheme hetereojunctions with in-built metal-redox for high performance photo-degradation of sulfamethoxazole and electrochemical dopamine detection. Environmental Research, 2021, 197, 111074.	7.5	58
76	Aerogels and metal–organic frameworks for environmental remediation and energy production. Environmental Chemistry Letters, 2018, 16, 797-820.	16.2	57
77	Recent advances on nickel nano-ferrite: A review on processing techniques, properties and diverse applications. Chemical Engineering Research and Design, 2021, 175, 182-208.	5.6	57
78	A novel nanocomposite of polyaniline and Fe0.01Ni0.01Zn0.98O: Photocatalytic, electrical and antibacterial properties. Journal of Alloys and Compounds, 2013, 578, 249-256.	5.5	56
79	Molecular Simulations Reveal the Mechanism and the Determinants for Ampicillin Translocation through OmpF. Journal of Physical Chemistry B, 2010, 114, 9608-9616.	2.6	54
80	Honeycomb structured activated carbon synthesized from Pinus roxburghii cone as effective bioadsorbent for toxic malachite green dye. Journal of Water Process Engineering, 2019, 32, 100931.	5.6	53
81	Optimal positioning of dynamic wireless charging infrastructure in a road network for battery electric vehicles. Transportation Research, Part D: Transport and Environment, 2020, 85, 102385.	6.8	53
82	Particle size characteristics of suspended sediment transported in meltwater from the Gangotri Glacier, central Himalaya — An indicator of subglacial sediment evacuation. Geomorphology, 2010, 122, 140-152.	2.6	52
83	Synthesis and characterization of novel Fe@ZnO nanosystem. Journal of Alloys and Compounds, 2013, 578, 235-241.	5.5	52
84	Assessment and review of hydrometeorological aspects for cloudburst and flash flood events in the third pole region (Indian Himalaya). Polar Science, 2018, 18, 5-20.	1.2	52
85	Carbon nitride, metal nitrides, phosphides, chalcogenides, perovskites and carbides nanophotocatalysts for environmental applications. Environmental Chemistry Letters, 2019, 17, 655-682.	16.2	51
86	lce-dams, outburst floods, and movement heterogeneity of glaciers, Karakoram. Global and Planetary Change, 2019, 180, 100-116.	3.5	50
87	Nanostructured magnetic inverse spinel Ni–Zn ferrite as environmental friendly visible light driven photo-degradation of levofloxacin. Chemical Engineering Research and Design, 2021, 175, 85-101.	5.6	50
88	Solar active nano-Zn1â^'xMgxFe2O4 as a magnetically separable sustainable photocatalyst for degradation of sulfadiazine antibiotic. Journal of Molecular Liquids, 2019, 294, 111574.	4.9	48
89	Facile fabrication of Zr2Ni1Cu7 trimetallic nano-alloy and its composite with Si3N4 for visible light assisted photodegradation of methylene blue. Journal of Molecular Liquids, 2018, 272, 170-179.	4.9	46
90	Laccase-assisted surface functionalization of lignocellulosics. Journal of Molecular Catalysis B: Enzymatic, 2014, 102, 48-58.	1.8	43

#	Article	IF	CITATIONS
91	The hazardous 2017–2019 surge and river damming by Shispare Glacier, Karakoram. Scientific Reports, 2020, 10, 4685.	3.3	43
92	Climatic control on extreme sediment transfer from Dokriani Glacier during monsoon, Garhwal Himalaya (India). Journal of Earth System Science, 2014, 123, 109-120.	1.3	42
93	A multifunctional nanocomposite pectin thorium(IV) tungstomolybdate for heavy metal separation and photoremediation of malachite green. Desalination and Water Treatment, 2016, 57, 19443-19455.	1.0	42
94	Determination of water quality of Ganga River System in Himalayan region, referencing indexing techniques. Arabian Journal of Geosciences, 2020, 13, 1.	1.3	42
95	Review on polycyclic aromatic hydrocarbons (PAHs) migration from wastewater. Journal of Contaminant Hydrology, 2021, 236, 103715.	3.3	42
96	Acceleration of photo-reduction and oxidation capabilities of Bi4O5I2/SPION@calcium alginate by metallic Ag: Wide spectral removal of nitrate and azithromycin. Chemical Engineering Journal, 2021, 423, 130173.	12.7	41
97	Nickel sulphide nano-composite assisted hole transport in thin film polymer solar cells. Solar Energy, 2020, 195, 310-317.	6.1	39
98	Meltwater storage and delaying characteristics of Gangotri Glacier (Indian Himalayas) during ablation season. Hydrological Processes, 2011, 25, 159-166.	2.6	38
99	Tracing isotopic signatures (ÎƊ and δ18O) in precipitation and glacier melt over Chorabari Glacier–Hydroclimatic inferences for the Upper Ganga Basin (UGB), Garhwal Himalaya. Journal of Hydrology: Regional Studies, 2018, 15, 68-89.	2.4	38
100	Pectin-guar gum-zinc oxide nanocomposite enhances human lymphocytes cytotoxicity towards lung and breast carcinomas. Materials Science and Engineering C, 2018, 90, 494-503.	7.3	38
101	Evolution of debris flow and moraine failure in the Gangotri Glacier region, Garhwal Himalaya: Hydro-geomorphological aspects. Geomorphology, 2019, 333, 152-166.	2.6	38
102	Carboxymethyl cellulose structured nano-adsorbent for removal of methyl violet from aqueous solution: isotherm and kinetic analyses. Cellulose, 2020, 27, 3677-3691.	4.9	38
103	Utilization of Ag2O–Al2O3–ZrO2 decorated onto rGO as adsorbent for the removal of Congo red from aqueous solution. Environmental Research, 2021, 197, 111179.	7.5	38
104	Characterization of suspended sediment in Meltwater from Glaciers of Garhwal Himalaya. Hydrological Processes, 2014, 28, 969-979.	2.6	37
105	Assessment of Heavy Metals Toxicity and Ecological Impact on Surface Water Quality Using HPI in Ganga River. INAE Letters, 2018, 3, 123-129.	1.0	37
106	Higher efficiency of <scp>ISSR</scp> markers over plastid <i>psbAâ€ŧrnH</i> region in resolving taxonomical status of genus <i>Ocimum</i> L Ecology and Evolution, 2016, 6, 7671-7682.	1.9	36
107	Routing aspects of electric vehicle drivers and their effects on network performance. Transportation Research, Part D: Transport and Environment, 2016, 46, 246-266.	6.8	36
108	Water Quality and Planktonic Composition of River Henwal (India) Using Comprehensive Pollution Index and Biotic-Indices. , 2020, 5, 541-553.		36

#	Article	IF	CITATIONS
109	Surface functionalization of coconut fibers by enzymatic biografting of syringaldehyde for the development of biocomposites. RSC Advances, 2015, 5, 76844-76851.	3.6	35
110	Chemical composition, genetic diversity, antibacterial, antifungal and antioxidant activities of camphor-basil (Ocimum kilimandscharicum Guerke). Industrial Crops and Products, 2018, 118, 246-258.	5.2	35
111	Designing of bentonite based nanocomposite hydrogel for the adsorptive removal and controlled release of ampicillin. Journal of Molecular Liquids, 2020, 319, 114166.	4.9	35
112	Intramolecular relaxation dynamics in semiflexible dendrimers. Journal of Chemical Physics, 2011, 134, 214901.	3.0	34
113	Guaran-based biodegradable and conducting interpenetrating polymer network composite hydrogels for adsorptive removal of methylene blue dye. Polymer Degradation and Stability, 2015, 122, 52-65.	5.8	34
114	Local surface plasmon resonance assisted energy harvesting in thin film organic solar cells. Journal of Alloys and Compounds, 2021, 856, 158172.	5.5	33
115	Dynamics of Semiflexible Dendrimers in Dilute Solutions. Macromolecules, 2010, 43, 7378-7385.	4.8	32
116	Thermo-mechanically stable sustainable polymer based solid electrolyte membranes for direct methanol fuel cell applications. Journal of Membrane Science, 2017, 526, 348-354.	8.2	32
117	Enhanced CO <sub>2</sub> Adsorption and Separation in Ionic-Liquid-Impregnated Mesoporous Silica MCM-41: A Molecular Simulation Study. Journal of Physical Chemistry C, 2018, 122, 8216-8227.	3.1	32
118	Mg0.5NixZn0.5-xFe2O4 spinel as a sustainable magnetic nano-photocatalyst with dopant driven band shifting and reduced recombination for visible and solar degradation of Reactive Blue-19. Advanced Powder Technology, 2020, 31, 4585-4597.	4.1	32
119	Comparative study on seasonal variation in hydro-chemical parameters of Ganga River water using comprehensive pollution index (CPI) at Rishikesh, (Uttarakhand) India. , 0, 118, 87-95.		32
120	A Perspective on Rishiganga-Dhauliganga Flash Flood in the Nanda Devi Biosphere Reserve, Garhwal Himalaya, India. Journal of the Geological Society of India, 2021, 97, 335-338.	1.1	31
121	Molar volume, viscosity and conductance studies of some alkali metal chlorides in aqueous ascorbic acid. Journal of Molecular Liquids, 2009, 150, 39-42.	4.9	30
122	Cellulose Nanocrystal Templated Graphene Nanoscrolls for High Performance Supercapacitors and Hydrogen Storage: An Experimental and Molecular Simulation Study. Scientific Reports, 2018, 8, 3886.	3.3	30
123	Graphene oxide supported La/Co/Ni trimetallic nano-scale systems for photocatalytic remediation of 2-chlorophenol. Journal of Molecular Liquids, 2019, 294, 111605.	4.9	30
124	Integrated Valorization of Desalination Brine through NaOH Recovery: Opportunities and Challenges. Angewandte Chemie - International Edition, 2019, 58, 6502-6511.	13.8	30
125	LaTiO2N/Bi2S3 Z-scheme nano heterostructures modified by rGO with high interfacial contact for rapid photocatalytic degradation of tetracycline. Journal of Molecular Liquids, 2020, 311, 113300.	4.9	30
126	Facile and One-Step in Situ Synthesis of Pure Phase Mesoporous Li <sub>2</sub> MnSiO <sub>4</sub> /CNTs Nanocomposite for Hybrid Supercapacitors. ACS Applied Energy Materials, 2020, 3, 2450-2464.	5.1	30

#	Article	IF	CITATIONS
127	Hydroclimatic influence on particle size distribution of suspended sediments evacuated from debris-covered Chorabari Glacier, upper Mandakini catchment, central Himalaya. Geomorphology, 2016, 265, 45-67.	2.6	29
128	Hydrometeorological assessments and suspended sediment delivery from a central Himalayan glacier in the upper Ganga basin. International Journal of Sediment Research, 2018, 33, 493-509.	3.5	29
129	Topographic and climatic influence on seasonal snow cover: Implications for the hydrology of ungauged Himalayan basins, India. Journal of Hydrology, 2020, 585, 124716.	5.4	29
130	Utilizing recycled LiFePO4 from batteries in combination with B@C3N4 and CuFe2O4 as sustainable nano-junctions for high performance degradation of atenolol. Chemosphere, 2018, 209, 457-469.	8.2	29
131	Investigation of structural and magnetic properties of thermal plasma-synthesized Fe1â^'xNi alloy nanoparticles. Journal of Alloys and Compounds, 2016, 663, 30-40.	5.5	28
132	Conformational transitions in semiflexible dendrimers induced by bond orientations. Journal of Chemical Physics, 2012, 137, 124903.	3.0	27
133	Gum Acaciaâ€ <i>cl</i> â€poly(acrylamide)@carbon nitride Nanocomposite Hydrogel for Adsorption of Ciprofloxacin and its Sustained Release in Artificial Ocular Solution. Macromolecular Materials and Engineering, 2020, 305, 2000274.	3.6	27
134	Electrospun ferric ceria nanofibers blended with MWCNTs for high-performance electrochemical detection of uric acid. Ceramics International, 2020, 46, 9050-9064.	4.8	26
135	AgO/MgO/FeO@Si3N4 nanocomposite with robust adsorption capacity for tetracycline antibiotic removal from aqueous system. Advanced Powder Technology, 2020, 31, 4310-4318.	4.1	26
136	A fractional model to describe the Brownian motion of particles and its analytical solution. Advances in Mechanical Engineering, 2015, 7, 168781401561887.	1.6	25
137	The development of antibacterial and hydrophobic functionalities in natural fibers for fiber-reinforced composite materials. Journal of Environmental Chemical Engineering, 2016, 4, 1743-1752.	6.7	25
138	Surface functionalization of lignin constituent of coconut fibers via laccase-catalyzed biografting for development of antibacterial and hydrophobic properties. Journal of Cleaner Production, 2016, 113, 176-182.	9.3	25
139	Character-based DNA barcoding for authentication and conservation of IUCN Red listed threatened species of genus Decalepis (Apocynaceae). Scientific Reports, 2017, 7, 14910.	3.3	25
140	Fabrication of oxidized graphite supported La2O3/ZrO2 nanocomposite for the photoremediation of toxic fast green dye. Journal of Molecular Liquids, 2019, 277, 738-748.	4.9	25
141	Ag0-Ag2O embedded nanocomposite hydrogel for adsorption-coupled-photocatalytic removal of triclosan. Materials Letters, 2020, 276, 128169.	2.6	25
142	Constructing Z-scheme LaTiO2N/g-C3N4@Fe3O4 magnetic nano heterojunctions with promoted charge separation for visible and solar removal of indomethacin. Journal of Water Process Engineering, 2020, 36, 101391.	5.6	25
143	Analysis of Climate and Melt-runoff in Dunagiri Glacier of Garhwal Himalaya (India). Water Resources Management, 2014, 28, 3035-3055.	3.9	24
144	A day-to-day dynamical model for the evolution of path flows under disequilibrium of traffic networks with fixed demand. Transportation Research Part B: Methodological, 2015, 80, 235-256.	5.9	24

#	Article	IF	CITATIONS
145	Hydroclimatic significance of stable isotopes in precipitation from glaciers of <scp>Garhwal Himalaya</scp> , <scp>Upper Ganga Basin</scp> ( <scp>UGB</scp> ), <scp>India</scp> . Hydrological Processes, 2018, 32, 1874-1893.	2.6	24
146	Evaluation of single and multilocus DNA barcodes towards species delineation in complex tree genus Terminalia. PLoS ONE, 2017, 12, e0182836.	2.5	24
147	Essential oil composition of four <i>Ocimum</i> spp. from the Peninsular India. Journal of Essential Oil Research, 2016, 28, 35-41.	2.7	23
148	Facile fabrication of chitosan-cl-poly(AA)/ZrPO4 nanocomposite for remediation of rhodamine B and antimicrobial activity. Journal of King Saud University - Science, 2020, 32, 1359-1365.	3.5	23
149	Feasibility of nuclear ribosomal region ITS1 over ITS2 in barcoding taxonomically challenging genera of subtribe Cassiinae (Fabaceae). PeerJ, 2016, 4, e2638.	2.0	22
150	Asymptomatic Plasmodium malariae infections in children from suburban areas of Yaoundé, Cameroon. Parasitology International, 2018, 67, 29-33.	1.3	22
151	Environmental friendly and robust Mg0.5-xCuxZn0.5Fe2O4 spinel nanoparticles for visible light driven degradation of Carbamazepine: Band shift driven by dopants. Materials Letters, 2021, 284, 129005.	2.6	22
152	Recent progress and challenges in photocatalytic water splitting using layered double hydroxides (LDH) based nanocomposites. International Journal of Hydrogen Energy, 2022, 47, 37438-37475.	7.1	22
153	Caustic Soda Production, Energy Efficiency, and Electrolyzers. ACS Energy Letters, 2021, 6, 3563-3566.	17.4	21
154	Entropy weighted average method for the determination of a single representative path flow solution for the static user equilibrium traffic assignment problem. Transportation Research Part B: Methodological, 2015, 71, 213-229.	5.9	20
155	Micropropagation, encapsulation, and conservation of Decalepis salicifolia, a vanillin isomer containing medicinal and aromatic plant. In Vitro Cellular and Developmental Biology - Plant, 2020, 56, 526-537.	2.1	20
156	Delineation of Ocimum gratissimum L. complex combining morphological, molecular and essential oils analysis. Industrial Crops and Products, 2019, 139, 111536.	5.2	19
157	Population Dynamics and Conservation Implications of Decalepis arayalpathra (J. Joseph and V.) Tj ETQq1 1 0.784 Biotechnology, 2015, 176, 1413-1430.	314 rgBT 2.9	/Overlock 10 18
158	Exclusion of Organic Dye Using Neoteric Activated Carbon Prepared from <i>Cornulaca</i> <i>monacantha</i> Stem: Equilibrium and Thermodynamics Studies. Materials Science Forum, 0, 875, 1-15.	0.3	18
159	Sustainable Approach for Mechanical Recycling of Poly(lactic acid)/Cellulose Nanocrystal Films: Investigations on Structure–Property Relationship and Underlying Mechanism. Industrial & Engineering Chemistry Research, 2018, 57, 14493-14508.	3.7	18
160	Orientational relaxation in semiflexible dendrimers. Physical Chemistry Chemical Physics, 2013, 15, 20294.	2.8	17
161	Glacier changes in Upper Tons River basin, Garhwal Himalaya, Uttarakhand, India. Zeitschrift Für Geomorphologie, 2013, 57, 225-244.	0.8	17
162	Chemical composition of root aroma of <i>Decalepisarayalpathra</i> (J. Joseph and V.) Tj ETQq0 0 0 rgBT	Overlock 1.8	10 Tf 50 67 1 17

Natural Product Research, 2014, 28, 1202-1205.

#	Article	IF	CITATIONS
163	Visibly Active FeO/ZnO@PANI Magnetic Nano-photocatalyst for the Degradation of 3-Aminophenol. Topics in Catalysis, 2020, 63, 1302-1313.	2.8	17
164	ISSR-Derived Species-Specific SCAR Marker for Rapid and Accurate Authentication of Ocimum tenuiflorum L. Planta Medica, 2018, 84, 117-122.	1.3	16
165	Preparation and Characterization of Gum Acacia/Ce(IV)MoPO4 Nanocomposite Ion Exchanger for Photocatalytic Degradation of Methyl Violet Dye. Journal of Inorganic and Organometallic Polymers and Materials, 2019, 29, 1171-1183.	3.7	16
166	Fe3O4 mediated Z-scheme BiVO4/Cr2V4O13 strongly coupled nano-heterojunction for rapid degradation of fluoxetine under visible light. Materials Letters, 2020, 281, 128650.	2.6	16
167	Potential seismic precursors and surficial dynamics of a deadly Himalayan disaster: an early warning approach. Scientific Reports, 2022, 12, 3733.	3.3	16
168	Sodium Dodecyl Sulphate-Supported Nanocomposite as Drug Carrier System for Controlled Delivery of Ondansetron. International Journal of Environmental Research and Public Health, 2018, 15, 414.	2.6	15
169	Multi-criteria based approach to identify critical links in a transportation network. Case Studies on Transport Policy, 2019, 7, 519-530.	2.5	15
170	Organic matter priming by invasive plants depends on dominant mycorrhizal association. Soil Biology and Biochemistry, 2020, 140, 107645.	8.8	14
171	Advances and challenges in metal ion separation from water. Trends in Chemistry, 2021, 3, 819-831.	8.5	14
172	Fe/La/Zn nanocomposite with graphene oxide for photodegradation of phenylhydrazine. Journal of Molecular Liquids, 2019, 285, 362-374.	4.9	13
173	Practical scale up synthesis of carboxylic acids and their bioisosteres 5-substituted-1 <i>H</i> -tetrazoles catalyzed by a graphene oxide-based solid acid carbocatalyst. RSC Advances, 2021, 11, 11166-11176.	3.6	13
174	Investigating reaction pathways in rare events simulations of antibiotics diffusion through protein channels. Journal of Molecular Modeling, 2010, 16, 1701-1708.	1.8	12
175	Intramolecular relaxation of flexible dendrimers with excluded volume. Journal of Chemical Physics, 2014, 141, 034902.	3.0	12
176	Dynamics of dendrimers with excluded volume: A comparison with experiments and simulations. Journal of Rheology, 2016, 60, 111-120.	2.6	12
177	Ggum-poly(Itaconic Acid) Based Superabsorbents Via Two-Step Free-Radical Aqueous Polymerization for Environmental and Antibacterial Applications. Journal of Polymers and the Environment, 2017, 25, 176-191.	5.0	12
178	Metallic and bimetallic phosphides-based nanomaterials for photocatalytic hydrogen production and water detoxification: a review. Environmental Chemistry Letters, 2022, 20, 597-632.	16.2	12
179	Conformation and intramolecular relaxation dynamics of semiflexible randomly hyperbranched polymers. Journal of Chemical Physics, 2013, 138, 104902.	3.0	11
180	Emergence of sulfadoxine–pyrimethamine resistance in Indian isolates of Plasmodium falciparum in the last two decades. Infection, Genetics and Evolution, 2015, 36, 190-198.	2.3	11

#	Article	IF	CITATIONS
181	When and where should there be dedicated lanes under mixed traffic of automated and human-driven vehicles for system-level benefits?. Research in Transportation Business and Management, 2020, 36, 100527.	2.9	11
182	Effect of salt stress on seed germination, morphology, biochemical parameters, genomic template stability, and bioactive constituents of Andrographis paniculata Nees. Acta Physiologiae Plantarum, 2021, 43, 1.	2.1	11
183	SLOPE-BASED PATH SHIFT PROPENSITY ALGORITHM FOR THE STATIC TRAFFIC ASSIGNMENT PROBLEM. International Journal for Traffic and Transport Engineering, 2014, 4, 297-319.	0.4	11
184	Update Strategies for Restricted Master Problems for User Equilibrium Traffic Assignment Problem. Transportation Research Record, 2012, 2283, 131-142.	1.9	10
185	Estimation of snow/glacier melt contribution in the upper part of the Beas River basin, Himachal Pradesh, using conventional and SNOWMOD modeling approach. Journal of Water and Climate Change, 2015, 6, 880-890.	2.9	10
186	Slope-Based Multipath Flow Update Algorithm for Static User Equilibrium Traffic Assignment Problem. Transportation Research Record, 2010, 2196, 1-10.	1.9	9
187	Semiflexibility induced range of conformations in dendrimers. Soft Matter, 2013, 9, 2375.	2.7	9
188	Surface Functionalization of Sisal Fibers Using Peroxide Treatment Followed by Grafting of Poly(ethyl acrylate) and Copolymers. International Journal of Polymer Analysis and Characterization, 2013, 18, 596-607.	1.9	9
189	Energetics of Preferential Binding of Retinoic Acid-Inducible Gene-I to Double-Stranded Viral RNAs with 5′ Tri-/Diphosphate over 5′ Monophosphate. ACS Omega, 2018, 3, 3786-3795.	3.5	9
190	Genetic profiling of the Plasmodium falciparum parasite population in uncomplicated malaria from India. Malaria Journal, 2019, 18, 385.	2.3	9
191	A simplified framework for sequencing of transportation projects considering user costs and benefits. Transportmetrica A: Transport Science, 2018, 14, 346-371.	2.0	8
192	ISSR Characterization and Quantification of Purpurin and Alizarin in Rubia cordifolia L. Populations from India. Biochemical Genetics, 2019, 57, 56-72.	1.7	8
193	Integrated Valorization of Desalination Brine through NaOH Recovery: Opportunities and Challenges. Angewandte Chemie, 2019, 131, 6570-6579.	2.0	8
194	Ag2O–Al2O3–ZrO2 Trimetallic Nanocatalyst for High Performance Photodegradation of Nicosulfuron Herbicide. Topics in Catalysis, 2020, 63, 1272-1285.	2.8	8
195	DNA barcode based species-specific marker for Ocimum tenuiflorum and its applicability in quantification of adulteration in herbal formulations using qPCR. Journal of Herbal Medicine, 2020, 23, 100376.	2.0	8
196	Graft Copolymerization of Acrylonitrile and Ethyl Acrylate onto <i>Pinus Roxburghii</i> Wood Surface Enhanced Physicochemical Properties and Antibacterial Activity. Journal of Chemistry, 2020, 2020, 1-16.	1.9	8
197	Pentafluoropyridine functionalized novel heteroatom-doped with hierarchical porous 3D cross-linked graphene for supercapacitor applications. RSC Advances, 2021, 11, 26892-26907.	3.6	8
198	Adventitious root cultures of Decalepis salicifolia for the production of 2-hydroxy-4-methoxybenzaldehyde, a vanillin isomer flavor metabolite. Applied Microbiology and Biotechnology, 2021, 105, 3087-3099.	3.6	8

#	Article	IF	CITATIONS
199	CO2 Reforming of CH4 on Mesoporous Alumina-Supported Cobalt Catalyst: Optimization of Lanthana Promoter Loading. Topics in Catalysis, 2021, 64, 338-347.	2.8	8
200	Characteristics of surge-type tributary glaciers, Karakoram. Geomorphology, 2022, 403, 108161.	2.6	8
201	Effect of excluded volume on the rheology and transport dynamics of randomly hyperbranched polymers. Journal of Chemical Physics, 2015, 142, 174906.	3.0	7
202	Structure-Based Energetics of Stop Codon Recognition by Eukaryotic Release Factor. Journal of Chemical Information and Modeling, 2017, 57, 2321-2328.	5.4	7
203	Principles of tRNA <sup>Ala</sup> Selection by Alanyl–tRNA Synthetase Based on the Critical G3·U70 Base Pair. ACS Omega, 2019, 4, 15539-15548.	3.5	7
204	Ion transfer channel network formed by flower and rod shape crystals of hair hydrolysate in poly(vinyl alcohol) matrix and its application as anion exchange membrane in fuel cells. Journal of Colloid and Interface Science, 2021, 587, 214-228.	9.4	7
205	Stage-Discharge Relationship. Encyclopedia of Earth Sciences Series, 2011, , 1079-1081.	0.1	7
206	Challenges to CV and AV Applications in Truck Freight Operations. , 2017, , .		7
207	Strategies to Enhance the Performance of Pathâ€Based Static Traffic Assignment Algorithms. Computer-Aided Civil and Infrastructure Engineering, 2014, 29, 330-341.	9.8	6
208	Molecular profiling of fungal assemblages in the healthy and infected roots of Decalepis arayalpathra (J. Joseph & V. Chandras) Venter, an endemic and endangered ethnomedicinal plant from Western Ghats, India. Annals of Microbiology, 2015, 65, 785-797.	2.6	6
209	Transportation Investment Decision Making for Medium to Large Transportation Networks. Transportation in Developing Economies, 2016, 2, 1.	1.6	6
210	Morphology-dependent performance of thin film organic solar cells. Journal of Modern Optics, 2019, 66, 399-406.	1.3	6
211	Morpho-genetic divergence and population structure in Indian Santalum album L Trees - Structure and Function, 2020, 34, 1113-1129.	1.9	6
212	Analytical quality-by-design (AQbD) guided development of a robust HPLC method for the quantification of plumbagin from <i>Plumbago</i> species. Journal of Liquid Chromatography and Related Technologies, 2021, 44, 529-537.	1.0	6
213	Essential Oil Constituents of Alseodaphne semecarpifolia from Central Western Ghats, India. Chemistry of Natural Compounds, 2016, 52, 516-517.	0.8	5
214	Population Genetics Coupled Chemical Profiling for Conservation Implications of Decalepis salicifolia (Bedd. ex Hook.f.) Venter, an Endemic and Critically Endangered Species of Western Ghats, India. Biochemical Genetics, 2020, 58, 452-472.	1.7	5
215	Assessing the in vitro sensitivity with associated drug resistance polymorphisms in Plasmodium vivax clinical isolates from Delhi, India. Experimental Parasitology, 2021, 220, 108047.	1.2	5
216	Gone and forgotten: facilitative effects of intercropping combinations did not carry over to affect barley performance in a follow-up crop rotation. Plant and Soil, 2021, 467, 405-419.	3.7	5

#	Article	IF	CITATIONS
217	Thalictrum nainitalense (Ranunculaceae), a new species from the Uttarakhand Himalaya, India. Folia Geobotanica, 2018, 53, 449-455.	0.9	4
218	Principle of DNA recognition by sporulation-regulatory protein (Spo0A) in <i>Bacillus subtilis</i> . Journal of Biomolecular Structure and Dynamics, 2020, 38, 5186-5194.	3.5	4
219	Comparative analysis of Plasmodium falciparum dihydrofolate-reductase gene sequences from different regions of India. Heliyon, 2020, 6, e03715.	3.2	4
220	Timing matters: Distinct effects of nitrogen and phosphorus fertilizer application timing on root system architecture responses. Plant-Environment Interactions, 2021, 2, 194-205.	1.5	4
221	Time series analysis of hydrometeorological data for the characterization of meltwater storage in glaciers of Garhwal Himalaya. , 2021, , 373-388.		4
222	Assessment of water recharge source of geothermal systems in Garhwal Himalaya (India). Arabian Journal of Geosciences, 2021, 14, 1.	1.3	4
223	Early treatment failure in concurrent dengue and mixed malaria species infection with suspected resistance to artemisinin combination therapy from a tertiary care center in Delhi: a case report. International Medical Case Reports Journal, 2017, Volume 10, 289-294.	0.8	3
224	Systematic Position, Phylogeny, and Taxonomic Revision of Indian Ocimum. Compendium of Plant Genomes, 2018, , 61-72.	0.5	3
225	Evaluation of Ground Water Quality by Use of Water Quality Index in the Vicinity of the Rajaji National Park Haridwar, Uttarakhand, India. Springer Hydrogeology, 2021, , 343-356.	0.3	3
226	Decadal Response of Dokriani Glacier using High-resolution Hydrological Data, Indian Himalaya. Journal of the Geological Society of India, 2022, 98, 62-68.	1.1	3
227	<i>In vitro</i> sensitivity to antimalarial drugs and polymorphisms in <i>Pfg377</i> gene in <i>Plasmodium falciparum</i> field isolates from Mewat, India. Pathogens and Global Health, 2017, 111, 225-233.	2.3	2
228	Effect of Crossâ€Linker in Poly( N â€Isopropyl Acrylamide)â€Graftedâ€Gelatin Gels Prepared by Microwaveâ€Assisted Synthesis. ChemistrySelect, 2019, 4, 10346-10351.	1.5	2
229	Why double-stranded RNA with 5′-monophosphate is a poor binder to retinoic acid-inducible gene-l with respect to 5′-hydroxyl analogue?. Journal of Biomolecular Structure and Dynamics, 2020, 38, 4048-4055.	3.5	2
230	Skeletal Calsequestrin - Calcium Interaction: Role of Acidic C-Terminus. Biophysical Journal, 2013, 104, 173a.	0.5	1
231	Peroxide Treatment of Soy Protein Fibers Followed by Grafting of Poly(methyl acrylate) and Copolymers. Journal of Renewable Materials, 2013, 1, 302-310.	2.2	1
232	Theoretical analysis of natural gas recovery from marginal wells with a deep well reactor. AICHE Journal, 2017, 63, 3642-3650.	3.6	1
233	Suspended Sediment Load. Encyclopedia of Earth Sciences Series, 2011, , 1132-1132.	0.1	1
234	Fabrication and Characterization of Polysorbate/Ironmolybdophosphate Nanocomposite: Ion Exchange Properties and pH-responsive Drug Carrier System for Methylcobalamin. Current Analytical Chemistry, 2020, 16, 138-148.	1.2	1

#	Article	IF	CITATIONS
235	Geocryology. Encyclopedia of Earth Sciences Series, 2011, , 324-325.	0.1	Ο
236	DNA barcoding coupled with secondary structure information enhances Achyranthes species resolution. Journal of Applied Research on Medicinal and Aromatic Plants, 2020, 19, 100269.	1.5	0
237	Microbial fuel cell: a greener way to protect the environment. , 2021, , 575-584.		ο
238	Decalepis salicifolia (Bedd. ex Hook. f.) Venter: A steno-endemic and critically endangered medicinal and aromatic plant from Western Ghats, India. Journal of Biosciences, 2021, 46, 1.	1.1	0
239	U-Shape Valley. Encyclopedia of Earth Sciences Series, 2011, , 1217-1218.	0.1	Ο
240	Terraces. Encyclopedia of Earth Sciences Series, 2011, , 1155-1155.	0.1	0
241	Gravel Sheet. Encyclopedia of Earth Sciences Series, 2011, , 477-477.	0.1	Ο
242	Marginal Channel (Lateral Meltwater Channel). Encyclopedia of Earth Sciences Series, 2011, , 724-724.	0.1	0
243	Terminus. Encyclopedia of Earth Sciences Series, 2011, , 1154-1155.	0.1	Ο
244	Snowboard. Encyclopedia of Earth Sciences Series, 2011, , 1071-1071.	0.1	0
245	Glacioisostasy. Encyclopedia of Earth Sciences Series, 2011, , 439-440.	0.1	Ο
246	Seasonal Snow Cover. Encyclopedia of Earth Sciences Series, 2011, , 974-975.	0.1	0
247	Glacier Sediment Dynamics, Flux and Facies: A Perspective From the Indian Himalaya. , 2021, , .		0